



UNIVERSITY OF LEEDS

This is a repository copy of *Efficient and selective oxidation of sulfides in batch and continuous flow using styrene-based polymer immobilised ionic liquid phase supported peroxotungstates*.

White Rose Research Online URL for this paper:
<http://eprints.whiterose.ac.uk/104529/>

Version: Accepted Version

Article:

Doherty, S, Knight, JG, Carroll, MA et al. (6 more authors) (2016) Efficient and selective oxidation of sulfides in batch and continuous flow using styrene-based polymer immobilised ionic liquid phase supported peroxotungstates. RSC Advances, 6 (77). pp. 73118-73131.

<https://doi.org/10.1039/c6ra11157b>

© 2016, Royal Society of Chemistry. This is an author produced version of a paper published in RSC Advances. Uploaded in accordance with the publisher's self-archiving policy.

Reuse

Unless indicated otherwise, fulltext items are protected by copyright with all rights reserved. The copyright exception in section 29 of the Copyright, Designs and Patents Act 1988 allows the making of a single copy solely for the purpose of non-commercial research or private study within the limits of fair dealing. The publisher or other rights-holder may allow further reproduction and re-use of this version - refer to the White Rose Research Online record for this item. Where records identify the publisher as the copyright holder, users can verify any specific terms of use on the publisher's website.

Takedown

If you consider content in White Rose Research Online to be in breach of UK law, please notify us by emailing eprints@whiterose.ac.uk including the URL of the record and the reason for the withdrawal request.



eprints@whiterose.ac.uk
<https://eprints.whiterose.ac.uk/>

Efficient and Selective Oxidation of Sulphides in Batch and Continuous Flow using Styrene-Based Polymer Immobilised Ionic Liquid Phase Supported Peroxotungstates[†]

Received 00th January 20xx,
Accepted 00th January 20xx

DOI: 10.1039/x0xx00000x

www.rsc.org/

S. Doherty,^{*,a} J. G. Knight,^{*,a} M. A. Carroll,^a A. R. Clemmet,^a J. R. Ellison,^a T. Backhouse,^a N. Holmes^b and R. A. Bourne^b

Styrene-based peroxotungstate-modified polymer immobilized ionic liquid phase catalysts $[\text{PO}_4\{\text{WO}(\text{O}_2)_2\}_4]@\text{ImPIILP}$ (Im = imidazolium) are remarkably efficient systems for the selective oxidation of sulfides under mild conditions both in batch and as a segmented or continuous flow process using either ethanol or acetonitrile as solvent or mobile phase, respectively. The performance of these styrene-based systems has been compared against their Ring Opening Metathesis Polymerisation derived counterparts to assess their relative merits. A comparative survey revealed catalyst supported on *N*-benzyl imidazolium decorated polymer immobilised ionic liquid to be the most efficient and a cartridge packed with a mixture of $[\text{PO}_4\{\text{WO}(\text{O}_2)_2\}_4]@\text{ImPIILP}$ and silica operated as a segmented or continuous flow system giving good conversions and high selectivity for sulfoxide. The immobilised catalyst remained highly active for the sulfoxidation of thioanisole in ethanol with a stable conversion-selectivity profile for up to 8 h under continuous flow operation; for comparison conversions with a mixture of $[\text{NBu}_4]_3[\text{PO}_4\{\text{WO}(\text{O}_2)_2\}_4]$ and silica dropped dramatically after only 15 min as a result of rapid leaching while $[\text{PO}_4\{\text{WO}(\text{O}_2)_2\}_4]@\text{ImPIILP}$ prepared from commercially available Merrifield resin also gave consistently lower conversions; these benchmark comparisons serve to underpin the potential benefits of preparing the polymer immobilized ionic liquid supports.

Introduction

Sulfoxides and sulfones are technologically important compounds which find use as intermediates in the synthesis of fine chemicals, bioactive compounds, agrochemicals,¹ as chiral auxiliaries in asymmetric synthesis² and most recently as ligands for transition metal asymmetric catalysis.³ Sulfoxidation is also the basis for the catalytic oxidative desulfurisation of crude oil to remove sulfur-based impurities as the resulting sulfones can be selectively extracted into a polar solvent under milder conditions than those traditionally required for industrial catalytic hydrodesulfurisation.⁴ A variety of powerful oxidants have been employed for sulfoxidation including *m*-chloroperbenzoic acid,⁵ UHP,⁶ NaClO,⁷ NaIO₄,⁸ oxone⁹ KMnO₄¹⁰ and dimethyldioxirane¹¹, however, these systems often suffer from low activity and/or selectivity, poor thermal stability, protocols that require long reaction times and/or complex handling procedures as well as poor E-factors.¹² As such there has been considerable interest in developing systems that utilise hydrogen peroxide as the oxidant as it is economical, environmentally benign and readily available.¹³ In this regard, a number of systems based on iron,¹⁴ manganese,¹⁵ vanadium,¹⁶

titanium,¹⁷ ruthenium,¹⁸ molybdenum,¹⁹ tungsten,²⁰ tantalum,²¹ rhenium,²² zinc,²³ tin,²⁴ and copper²⁵ have been developed. In addition to utilising hydrogen peroxide as the oxidant, an efficient catalyst must also be highly selective for either sulfoxide or sulfone, cost effective, straightforward to prepare and easy to manipulate, operate under mild conditions across a wide range of substrates, have good long term stability and be easy to recover and recycle. Even though highly selective catalysts have been developed there is still a demand to identify alternative oxidation systems to address the remaining issues such as low activity and poor thermal stability, complicated and onerous catalyst recovery procedures and leaching of the active component as well as the need to improve green credentials.²⁶ Immobilization of an efficient oxidation catalyst onto the surface of a porous support, metal oxide, magnetic particle or polymer has been widely explored as a method to facilitate catalyst separation, recovery and reuse;²⁷ while such systems often suffer from slow reaction rates there have been reports of immobilisation resulting in an enhancement in catalyst activity and selectivity compared with its corresponding homogeneous counterpart.²⁸

Ionic liquids are an intriguing class of solvent that has been widely utilized for immobilisation of catalysts under homogeneous, liquid-liquid biphasic and liquid-solid (SILP) biphasic conditions, in some cases with remarkable success.²⁹ Recent endeavours in this area include highly selective sulfoxidations catalysed by a SILP system based on imidazolium modified SBA-15 and $[\text{MoO}(\text{O}_2)_2(\text{H}_2\text{O})_n]$,³⁰ a magnetically recoverable sulfoxidation catalyst based on magnetic nanoparticles entrapped in a tungstate-functionalised polyionic liquid,³¹ an eco-friendly protocol for the oxidation of sulphides to sulfones catalysed by V₂O₅ in $[\text{C}_{12}\text{mim}][\text{HSO}_4]$,³² efficient and selective sulfoxidation catalysed by peroxotungstates immobilised on multilayer ionic liquid brushes-modified silica³³

^aNUCAT, School of Chemistry, Bedson Building, Newcastle University, Newcastle upon Tyne, NE1 7RU, UK.

^bInstitute of Process Research & Development, School of Chemistry, University of Leeds, Woodhouse Lane, Leeds LS2 9JT, United Kingdom
E-mail: simon.doherty@ncl.ac.uk; Tel: +44 (0) 191 208 6537

[†] This paper is dedicated to the memory of Professor Malcolm H. Chisholm (FRS)
Electronic Supplementary Information (ESI) available: Synthesis and characterisation of imidazolium-based monomers **1a-c**, co-polymers **2a-c**, polymer immobilized peroxotungstates **3a-e**, TGA and DSC curves for **2a-c** and **3a-c**, SEM images, FTIR traces and X-ray photoelectron spectra for **3a-c**, characterisation data for sulfoxides and sulfones, details of catalysis, recycle experiments and graphs showing conversion-selectivity profiles as a function of residence time for $[\text{PO}_4\{\text{WO}(\text{O}_2)_2\}_4]@\text{PIILP}$ -catalysed sulfoxidations under segmented and continuous flow. See DOI: 10.1039/b000000x/

Other recent developments include selective oxidation of sulfides with H₂O₂ catalysed by heterogeneous ionic liquid-based polyoxometalates,³⁴ selective oxidation of sulphides with a sulfoacid-hexafluorotitanate(IV) bifunctional ionic liquid,³⁵ ionic liquid-mediated oxidation of sulphides to sulfoxides,³⁶ efficient eco-friendly selective oxidation of sulphides to sulfoxides with molecular oxygen catalysed by Mn(OAc)₂ in [C₁₂mim][NO₃],³⁷ rapid oxidation of sulfides by themoregulated polyoxometalate based ionic liquids,^{20b,38} selective and efficient desulfurization by amphiphilic polyoxometalate-based ionic liquid supported silica,³⁹ and heterogeneous selective sulfoxidation with polymeric ionic liquid nanogel-immobilised tungstate anions.⁴⁰

We have recently applied the concept of SILP-based technology to develop peroxotungstate-based Polymer Immobilised Ionic Liquid Phase (PIILP) oxidation catalysts in order to combine the favourable and tuneable properties of ionic liquids with the advantages of a solid porous support.⁴¹ Ring Opening Metathesis derived ionic liquid polymers were used to prepare the corresponding peroxotungstate-based PIILP catalyst, [PO₄{WO(O)₂}]₄@PIILP on the basis that the well-behaved functional group tolerant nature of ruthenium-catalysed living polymerisation would enable surface properties, ionic microenvironment, porosity and hydrophilicity to be modified and thereby catalyst-surface interactions, substrate accessibility and catalyst efficacy to be optimised in a rational and systematic manner. Gratifyingly, our initial foray in this area demonstrated that peroxotungstate immobilised on pyrrolidinium-decorated norbornene/cyclooctene copolymer was a remarkably efficient system for the selective oxidation of sulfides in batch and continuous flow. This was the first report of continuous flow sulfoxidation and despite the potential importance of this technology there are still relatively few examples in the academic literature. In this regard, following our initial disclosure Alemán and co-workers developed a Pt(II)-based visible light photocatalyst for the oxidation of sulfides both in batch and flow; the system gave complete chemoselectivity for sulfoxide but required long reaction times (10 h) to reach good conversions.⁴² We have now undertaken a comparison of the efficiency of our original system against a range of polystyrene-based polymer immobilised ionic liquid supported peroxotungstates in order to assess the relative merits of both reasoning that styrene-based monomers are easy to prepare and the corresponding polymers would be more cost effective and have good thermal and mechanical integrity. Herein we report the results of this comparison which demonstrates that styrene-based polymer immobilised ionic liquid phase supported peroxotungstates give high conversions and excellent sulfoxide selectivity under mild conditions, both in batch and under continuous flow operation using ethanol as the solvent or mobile phase, and that the most efficient system outperforms its ROMP-derived counterpart. Moreover, the remarkable stability of the performance-time profile allowed continuous flow operation to be maintained over extended periods of time with only a minor reduction in performance. As continuous flow processing of sulfoxidation has not been thoroughly investigated this study will provide a valuable

benchmark and platform for future developments in this key area.

Results and Discussion

Catalysts synthesis and batch catalysis

Imidazolium based styrene monomers **1a-c** (Figure 1a) were prepared by alkylation of the corresponding imidazole with the appropriate electrophile and isolated as spectroscopically pure crystalline solids after work up and purification. The immediate and obvious advantage associated with these styrene-based supports is the ease of monomer synthesis compared with the linear 4 step synthesis required to prepare pyrrolidinium-based norbornene monomers for the corresponding ROMP-derived system. Co-polymers **2a-c** (Figure 1b) were prepared by AIBN initiated radical polymerisation of **1a-c** with styrene in ethanol at 90 °C, isolated by precipitation into diethyl ether and characterised by a combination of elemental analysis, solution and solid state NMR spectroscopy, gel permeation chromatography (GPC), thermogravimetric analysis, scanning electron microscopy (SEM) and IR spectroscopy.

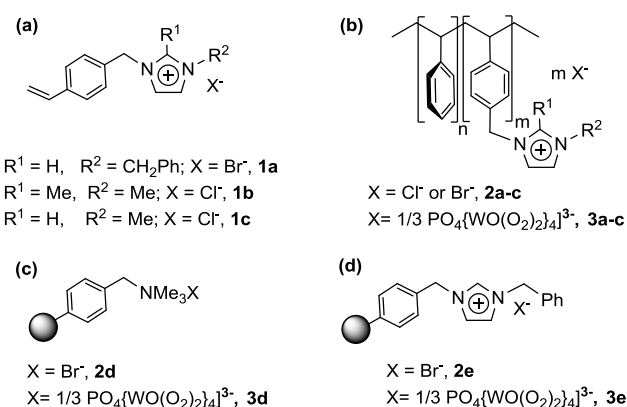


Fig. 1 (a) Imidazolium-based styrene monomers (b) polystyrene-based ionic copolymers (X = Cl⁻, Br⁻) used for the preparation of POM@ImPIILP **3a-c** (X = [PO₄{WO(O)₂}]₄]³⁻) (c) macroreticular resin **2d** and POM@PIILP **3d** and (d) imidazolium-modified Merrifield resin and POM@ImPIILP **3e**.

The molecular weight (*M_w*) of **2a-c** determined by gel permeation chromatography was measured to be 31,600 (**2a**), 26,100 (**2b**) 27,800 (**2c**) relative to polystyrene standards and the polydispersities of 1.32, 1.19, and 1.17, respectively, are consistent with relatively narrow monomodal molecular weight distributions. The ratio of imidazolium monomer to styrene incorporated into the polymer was determined to be ca. 0.5 which corresponds to m and n values of 32 and 16, respectively, based on the average molecular weights determined by GPC. The thermal stability of co-polymers **2a-c** was investigated by thermogravimetric analysis and differential scanning calorimetry. The TGA of **2a-c** showed an initial weight loss at ca. 100 °C, due to removal of physisorbed water and ethanol, followed by two main degradation pathways, indicating that the polymers are thermally stable up to 300 °C; this is well above

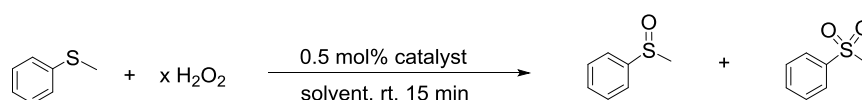
the reaction temperature required for liquid phase catalysis. Solution and solid state NMR spectra of **2a-c** confirm that the samples do not contain any imidazolium or styrene monomer as evidenced by the absence of signals at δ 5.2 and 5.8 ppm characteristic of vinylic protons. A reliable assignment of the signals in the solid state ^{13}C NMR spectrum of **2a-c** was obtained by conducting pairs of measurements, one with full cross-polarisation (dipolar dephasing with 0 μs delay) and one with a 50 μs dephasing delay to remove the CH and CH₂ signals; this enabled the quaternary and CH₃ signals to be identified.

Peroxotungstate-based PIILPs **3a-c** were prepared by stoichiometric exchange of the halide anion in **2a-c** with $[\text{PO}_4\{\text{WO}(\text{O}_2)_2\}_4]^{3-}$, generated by hydrogen peroxide-mediated decomposition of the heteropolyacid $\text{H}_3\text{PW}_{12}\text{O}_{40}$ (Figure 1b).⁴³ The desired product typically precipitated as an amorphous white solid and was characterised by a variety of techniques including solid state NMR spectroscopy, IR spectroscopy, TGA, SEM, XPS and elemental analysis. Decomposition of $\text{H}_3\text{PW}_{12}\text{O}_{40}$ into $[\text{PO}_4\{\text{WO}(\text{O}_2)_2\}_4]^{3-}$ was confirmed by a signal at δ 2.9 ppm in the solid state ^{31}P NMR spectrum; in the case of **3c** the spectrum also showed the presence of minor phosphorus-containing species previously identified by Hill and co-workers during their early studies on the formation, reactivity and stability of $[\text{PO}_4\{\text{WO}(\text{O}_2)_2\}_4]^{3-}$.⁴⁴ Surprisingly, TGA analysis revealed that thermal decomposition of **3a-c** occurred between 250-300 °C which is slightly lower than for **2a-c**; this may be associated with a reduction in the binding affinity due to the large size of the peroxotungstate anion compared with halide. A similar effect has recently been reported for a polymer ionic liquid nanogel-anchored tungstate which was less thermally stable than the corresponding parent polymeric ionic liquid nanogel.⁴⁰ Scanning electron microscopy revealed a stark difference in surface morphology of the polymers after loading of the peroxometalate (supporting information). Specifically, the surface of polyoxotungstate loaded **3a-c** exhibit a rough granular texture compared with the smooth flat surface of polymers **2a-c**. The X-ray photoelectron spectra of **3a-c** each contain characteristic W $4f_{7/2}$ and $4f_{5/2}$ doublets with binding energies of 37.1 and 39.1 eV, respectively, in good agreement with available literature data for tungsten ions in the +6 oxidation state.⁴⁴ The tungsten loadings of 32.0-35.0 wt% for **3a-c** were determined from elemental analytical data and are consistent with complete exchange of the bromide in **2a-c**. With the aim of comparing and evaluating the efficacy of in-house synthesised polymer immobilised ionic liquid supports **2a-c** against commercially available systems, $[\text{PO}_4\{\text{WO}(\text{O}_2)_2\}_4]^{3-}$ was

also supported on macroreticular resin **2d** and imidazolium-modified Merrifield resin **2e** (Scheme 1c-d).

A series of catalytic reactions were first conducted under batch conditions to establish optimum conditions for comparative catalyst evaluation, substrate screening and recycle experiments as well as to identify potential systems for use in developing a continuous flow process,⁴⁵ full details are presented in Table 1. Our initial optimisation focused on the sulfoxidation of thioanisole as the benchmark reaction as this oxidation has recently been catalysed by peroxometalate-based systems hosted in layered double hydroxides with enhanced activity and sulfoxide selectivity,²⁸ polyoxometalate-calix[4]arene hybrids,⁴⁶ thermoregulated Keggin-type polyoxometalate-based ionic liquids,^{20b,38} polymeric ionic liquids nanogels,⁴⁰ composite polyoxometalates supported on Fe_2O_3 ,⁴⁷ poly(ionic) liquid entrapped magnetic nanoparticles,³¹ and peroxometalates immobilised on the surface of ionic liquid modified silica.^{33,39} Gratifyingly, good conversions and high sulfoxide selectivity were obtained in methanol and ethanol after 15 min using a 0.5 mol% loading of **3a** at room temperature and a H_2O_2 : S mole ratio of 2.5 (entries 1-2). High selectivities were also achieved in propan-2-ol and ethylene glycol under the same conditions although reactions in the latter solvent were slower and elevated temperatures were required to achieve comparable conversions (entries 3-4). Slightly lower conversions were obtained in acetonitrile and 2-Me-THF, sulfoxide selectivity remained high (entries 5 and 6). For comparison the corresponding ROMP-based POM@PIILP system gave a slightly lower sulfoxide selectivity of 84% in acetonitrile, under the same conditions and at a similar conversion. In this regard, higher sulfoxide selectivity is generally obtained in protic solvents such as methanol and ethanol, which has been attributed to their high hydrogen-bonding capacity,^{27d,g,48} however, while alcohols are often the solvent of choice to achieve high sulfoxide selectivity, there have been recent reports in which acetonitrile has been identified as the optimum solvent.⁴⁹ The minor decrease in conversion with increasing alcohol carbon number (entries 1-3) may be associated with the different polymer swelling capacity of these solvents which could affect access of the substrate to the active site, however, the differences in conversion are relatively minor and any interpretation should be treated with caution. The high selectivity and conversion obtained in ethanol coupled with its green and sustainable credentials prompted us to use this solvent for the remaining optimisation studies.

Table 1 Oxidation of thioanisole as a function of catalyst, solvent and hydrogen peroxide ratio^a



entry	solvent	catalyst	H ₂ O ₂ equiv. x	Conversion ^b	% sulfoxide ^b	% Sulfone ^b	Sulfoxide selectivity ^{b,c}	TOF ^d
1	MeOH	3a	2.5	99	95	4	96	689
2	EtOH	3a	2.5	94	91	3	96	654
3	i-PrOH	3a	2.5	92	88	4	96	640
4	EG	3a	2.5	44	43	1	98	334
5	MeCN	3a	2.5	81	78	3	97	564
6	2-Me-THF	3a	2.5	54	44	2	96	376
7	EtOH	3a	2.0	76	74	3	98	528
8	EtOH	3a	3.0	95	91	3	96	661
9	EtOH	3a	4.0	100	91	9	91	696
10	EtOH	3a	5.0	100	83	17	83	696
11	EtOH ^f	-	2.5	0	-	-	-	-
12	EtOH	3b	2.5	25	25	0	100	173
13	MeCN	3b	2.5	49	48	1	98	336
14	EtOH	3c	2.5	36	35	1	99	234
15	MeCN	3c	2.5	53	52	1	99	359
16	EtOH	3d	2.5	5	5	0	100	39
17	MeCN	3d	2.5	18	17	1	94	125
18	EtOH	3e	2.5	57	56	1	99	403
19	MeCN	3e	2.5	42	41	1	99	297
20	EtOH	2a /H ₃ PW ₁₂ O ₄₀	2.5	2	2	0	100	19

^a Reaction conditions: 0.56–0.58 mol% **3a-e**, 1 mmol thioanisole, 1.0–3.0 mmol 35% H₂O₂, 3 mL solvent, 25 °C, 15 min. ^b Determined by ¹H NMR spectroscopy. ^c sulfoxide selectivity = [%sulfoxide/(%sulfoxide+%sulfone)] × 100%. ^d TOF = moles sulfide consumed per mole catalyst per hour. ^e Reaction conducted at 50 °C. ^f Reaction conducted without catalyst in the presence of 0.5 mol% **2a**.

Systematic variation of the H₂O₂: substrate mole ratio revealed that the best compromise between conversion and sulfoxide selectivity was obtained for a peroxide to substrate ratio of 2.5; below this ratio conversions were markedly lower (entry 7) while higher ratios gave complete consumption of sulphide but at the expense of selectivity which was markedly lower (entries 8–10). As sulfones are a useful class of compound the conversion-selectivity profile was also monitored as a function of temperature, with a peroxide to substrate ratio of 2.5, in order to identify conditions for the selective formation of methyl phenyl sulfone. Figure 2 shows that sulfoxide selectivity drops dramatically with increased temperature such that sulfone was obtained as the major product in 93% selectivity after 15 min at 328 K. A control reaction for the oxidation of thioanisole conducted in ethanol in the absence of peroxotungstate but with 0.5 mol% **2a** and 2.5 equivalents of H₂O₂ gave no conversion, which confirmed the active role of the catalyst (entry 11).

In order to explore the effect of the imidazolium cation on catalyst performance the efficiency of **3a-c** for the sulfoxidation of thioanisole in ethanol and acetonitrile was investigated under the optimum conditions identified above and compared with the corresponding systems prepared from commercially available resin **3d-e**, details of which are also summarised in Table 1 (entries 12–19). While **3a-c** all gave high sulfoxide

selectivities at room temperature in ethanol under optimum conditions, **3a** is the most active with a TOF of 654 h⁻¹ compared with 173 h⁻¹ and 234 h⁻¹ for **3b** and **3c**, respectively (entries 2, 12 and 14).

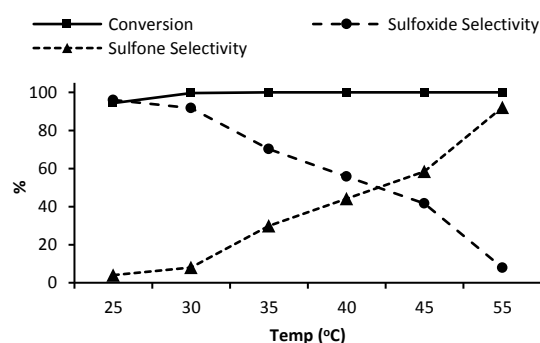
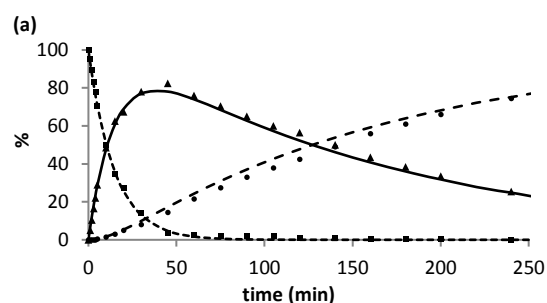


Fig. 2 Influence of temperature on selectivity and conversion for the sulfoxidation of thioanisole with H₂O₂ in ethanol using a 0.5 mol% loading of **3a**, a H₂O₂:S ratio of 2.5 and a reaction time of 15 min.

The data in Table 1 also highlights the merits of using catalyst prepared with in-house synthesised polymer immobilised



ionic liquids as **3d** and **3e** only reached 5% and 57% conversion, respectively, in ethanol which correspond to TOF's of 39 h⁻¹ and 403 h⁻¹, respectively, both of which are significantly lower than

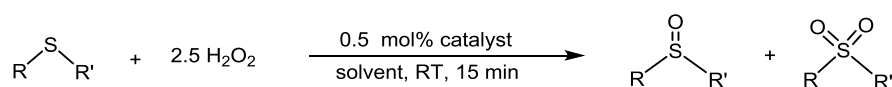
that of 654 h⁻¹ obtained with **3a** (entries 16 and 18). In contrast, even though **3a** was also more active than either **3b** or **3c** in acetonitrile, the difference in performance was not as marked as in ethanol, as evidenced by the TOF of 564 h⁻¹ for **3a** compared with 336 h⁻¹ and 359 h⁻¹ for **3b** and **3c**, respectively (entries 5, 13, 15). Gratifyingly, **3a-c** all outperformed **3d** by a considerable margin, even though the TOF of 125 h⁻¹ obtained in acetonitrile was a marked improvement on that in ethanol (entry 17). With the aim of investigating the possibility of generating [PO₄{WO(O₂)₂]₄]@ImPIILP *in situ* immediately prior to catalysis, in order to avoid the need to prepare, isolate and store the catalyst, H₃PW₁₂O₄₀ was supported on **2c** by wet impregnation from ethanol-water. Unfortunately, catalyst generated by treatment of the resulting H₃PW₁₂O₄₀/**2a** with hydrogen peroxide was essentially inactive for sulfoxidation of thioanisole in ethanol and only achieved 2% conversion under the same conditions in the same time (entry 20).

A comparative study of the variation in conversion against sulfoxide and sulfone as a function of time for the sulfoxidation of 4-nitrothioanisole catalysed by **3a** in ethanol and acetonitrile at room temperature shows that the composition-time profiles are qualitatively similar but that oxidation to sulfone is more rapid in acetonitrile than in ethanol (Figure 3). Approximate rate constants for the formation of methyl phenyl sulfoxide (*k_a*) and methyl phenyl sulfone (*k_b*) in ethanol and acetonitrile were extracted by fitting the concentration-time profile for the consumption of sulphide and the formation of product using pseudo steady state analysis. It should be noted that 2 equivalents of H₂O₂ are consumed during the reaction and as such the derived rate constants will only be meaningful for this comparison, even though the data fit is visually very good. The data confirms that the solvent has a more significant effect on the second oxidation compared with the first; this may be associated with the increased hydrogen bond capacity of ethanol which could solvate the H₂O₂ effectively and thereby reduce its availability at the catalyst as it becomes depleted and/or solvate the sulfoxide and thereby stabilise it with respect to further oxidation. However, catalyst solvation may also be responsible for the solvent dependent difference in *k_b* as it would be reasonable to expect solvation by ethanol to impede access of sulfoxide to the active centre to a greater extent than acetonitrile.

Table 2 Estimated rate constants for the formation of methyl phenyl sulfoxide (*k_a*) and methyl phenyl sulfone (*k_b*) in ethanol and acetonitrile^a

H ₂ O ₂	MeCN		EtOH	
	<i>k_a</i>	<i>k_b</i>	<i>k_a</i>	<i>k_b</i>
2.5	0.06	0.009	0.068	0.006

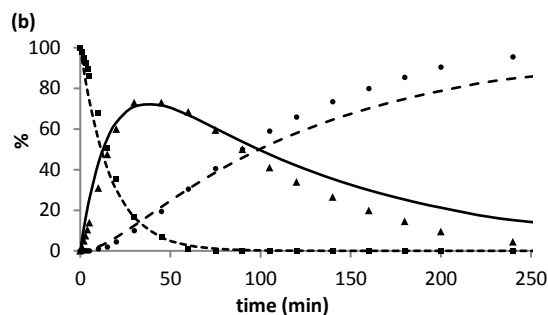
Table 3 Selective oxidation of sulfides to sulfoxides with hydrogen peroxide catalysed by [PO₄{WO(O₂)₂]₄]@ImPIILP (**3a-c**)^a



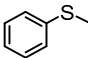
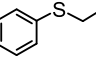
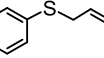
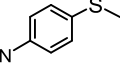
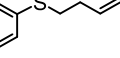
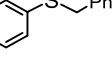
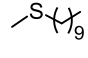
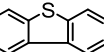
^a Data obtained using 4 mmol thioanisole, 12.2 mg **3a**, 12 mL solvent, 10 mmol H₂O₂ and monitored by analysing 0.2 mL aliquots over 250 min.

Fig. 3 Determination of rate constants for the formation of methyl phenyl sulfoxide (*k_a*) and methyl phenyl sulfone (*k_b*) by fitting the concentration-time profile for the consumption of sulfide and the formation of sulfoxide and sulfone in (a) in ethanol and (b) acetonitrile. Experimental data for sulphide (•), sulfoxide (▲) and sulfone (●); fitted data for sulphide (.....), sulfoxide (- - -) and sulfone (—).

Encouraged by the efficacy of **3a-c** for the selective oxidation of thioanisole, catalyst testing was extended to



explore their performance across a range of substrates under the optimum conditions identified above, full details of which are summarised in Table 3. The tabulated data clearly shows that **3a** outperforms both **3b** and **3c** across the entire range of substrates examined, in both ethanol and acetonitrile, as evidenced from the consistently higher conversions, however, it is more difficult to use selectivity as a parameter to compare performance as **3a-c** are all highly selective for sulfoxide within a relatively narrow range between 95-100%, albeit in some cases at low conversion. Interestingly, **3a** gave higher TOFs for sulfoxidation in ethanol compared with acetonitrile for all but one substrate; in contrast, **3b** and **3c** gave higher TOF's in acetonitrile than in ethanol for all substrates tested. Moreover, the performance of **3b** and **3c** is highly substrate specific with some quite marked differences in TOF. Interestingly, the difference in performance between **3a** and **3b-c** is most clearly manifested in ethanol as evidenced by the greater disparity in TOF's. The contrasting, disparate and solvent dependent conversions obtained even within this closely related series of catalysts highlights the complex nature of these PIILP systems, and, while it is not possible to identify a support-catalyst performance relationship at this stage, the data in Table 3 suggests that it may well be possible to tailor the ionic environment on the support to modify and optimise catalyst efficiency and enhance stability and longevity.

Substrate	Catalyst	Solvent	% Conversion ^b	% Sulfoxide ^b	% Sulfone ^b	% Sulfoxide selectivity ^{b,c}	TOF ^d
	3a	EtOH	94	91	3	97	654
	3b	EtOH	25	25	0	100	173
	3c	EtOH	34	34	1	99	58
	3a	MeCN	76	74	2	97	532
	3b	MeCN	49	48	1	98	337
	3c	MeCN	52	51	1	98	89
	3a	EtOH	85	82	3	96	594
	3b	EtOH	19.5	19	0.5	97	76
	3c	EtOH	27	26	1	97	182
	3a	MeCN	77	73	4	100	539
	3b	MeCN	49	48	1	99	260
	3c	MeCN	67	61	3	96	436
	3a	EtOH	75	73	2	98	525
	3b	EtOH	11	11	0	100	260
	3c	EtOH	15	15	0	100	102
	3a	MeCN	69	67	2	97	482
	3b	MeCN	38	36	2	96	76
	3c	MeCN	40	38	2	96	271
	3a	EtOH	37	36	1	96	258
	3b	EtOH	5	5	0	100	36
	3c	EtOH	7	7	0	100	52
	3a	MeCN	53	50	3	94	376
	3b	MeCN	23.5	23	0.5	98	167
	3c	MeCN	36	35	1	97	247
	3a	EtOH	65.5	64	1.5	98	459
	3b	EtOH	13.5	13	0.5	96	91
	3c	EtOH	16.5	16	0.5	97	111
	3a	MeCN	72	69	3	96	499
	3b	MeCN	64.5	62	2.5	96	449
	3c	MeCN	45.5	44	1.5	97	276
	3a	EtOH	59	57	2	97	474
	3b	EtOH	11	11	0	100	76
	3c	EtOH	15	15	0	100	108
	3a	MeCN	62	60	2	96	436
	3b	MeCN	48.5	47	1.5	97	336
	3c	MeCN	44	43	1	99	222
	3a	EtOH	100	95	5	95	697
	3b	EtOH	54.5	54	0.5	100	380
	3c	EtOH	69.5	69	0.5	100	473
	3a	MeCN	96	94	2	97	675
	3b	MeCN	89	87	2	98	618
	3c	MeCN	75	74	1	99	512
	3a^f	MeCN	41	32	9	79	143
	3b^f	MeCN	3	3	0	100	12
	3c^f	MeCN	18	13	5	71	63

^a Reaction conditions: 0.56-0.58 mol% **3a-c**, 1 mmol substrate, 2.5 mmol 35% H₂O₂, 3 mL solvent, 25 °C, 15 min. ^b Determined by ¹H NMR spectroscopy using 1,3-dinitrobenzene as internal standard. ^c sulfoxide selectivity = [%sulfoxide/(%sulfoxide+%sulfone)] × 100%. ^d TOF = moles sulfide consumed per mole of catalyst per hour. Average of 3 runs. ^e Determined by ¹³C NMR spectroscopy using 1,3-dinitrobenzene as internal standard. ^f Reaction conducted at 25 °C for 30 min

Not surprisingly, high TOFs were obtained for the sulfoxidation of n-decyl methyl sulfide in ethanol and acetonitrile with each

of the catalysts tested as this substrate is electron-rich and consequently easy to oxidise; as such it is not a reliable candidate for differentiating catalyst performance. The moderate to low conversions obtained for the [PO₄{WO(O₂)₂]₄]@ImPIILP-catalysed sulfoxidation of dibenzothiophene at room temperature in acetonitrile are consistent with the widely accepted electrophilic pathway and the lower nucleophilicity of this substrate; a recent

computational study also supports this pathway⁵⁰ as do numerous reports of increasing rates of oxidation with increasing nucleophilicity of the sulfide.^{20b,27d,48c,49} The TOF of 143 h⁻¹ obtained with **3a** at room temperature is a significant improvement on that of 9.6 h⁻¹ for a Merrifield resin supported peroxomolybdenum(VI) catalyst at 78 °C,^{27d} 25 h⁻¹ for oxodiperoxomolybdenum(VI) immobilised onto ionic liquid modified SBA-15,³⁰ 4 h⁻¹ for V₂O₅ in [C₁₂mim][HSO₄] at 45 °C³² and 40 h⁻¹ for a titanium cyclopentadienyl-silsesquioxane.^{17e} Unfortunately, it was not possible to obtain reliable data for the sulfoxidation of dibenzothiophene in ethanol due to its low solubility in this solvent. Oxidation of allylphenyl sulfide and homoallylphenyl sulfide occurred with complete chemoselectivity for sulfoxide and sulfone with no evidence for epoxidation of the double bond; this is most likely due to the mild conditions and short reaction times.^{19b,20c,27b,d}

Reassuringly, the optimum selectivities and TOFs in Table 3 either compete with or are an improvement on those of other immobilised polyoxo- or peroxometalate-based systems such as modified Merrifield resin supported peroxomolybdenum(VI),^{27b} modified SBA-15-based tungstates,^{27a} polyoxometalates hosted in layered double hydroxides,²⁸ polymeric ionic liquid nanogel-anchored tungstates,⁴⁰ a divanadium-substituted phosphotungstate supported on Fe₂O₃,⁴⁸ poly(acrylonitrile)-immobilised peroxotungstate,^{27d} tungstate-based poly(ionic liquid) entrapped magnetic nanoparticles³¹ and peroxotungstates immobilised on multilayer ionic liquid brushes-modified silica.^{27c} We believe that catalysts **3a-c** most likely operate via a three-step mechanism involving (i) rate determining attack of sulfide at polymer immobilised ionic liquid supported peroxotungstate (I) to afford (II), (ii) sulfoxide dissociation to generate tungsten-oxo (III) and (iii) catalyst regeneration (Figure 4). As such it should therefore be possible to control factors that influence catalyst efficacy such as the accessibility of the active site, the electrophilicity of the active peroxotungstate and catalyst stability by modifying the ionic microenvironment of the polymer immobilised ionic liquid support or introducing additional functional groups and cross linking.

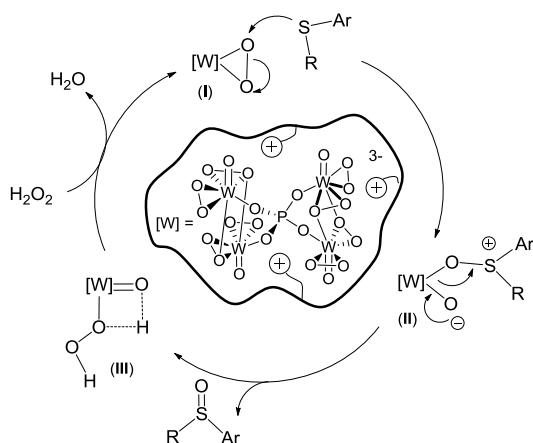
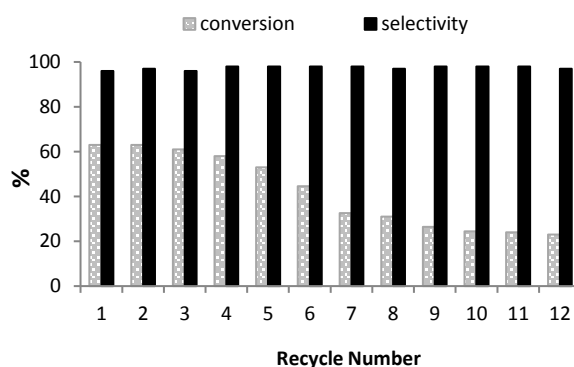


Fig. 4 Recycle study for the sulfoxidation of thioanisole in ethanol catalysed by [PO₄{WO(O₂)₂]₄]@ImPIILP (**3a-c**).

Catalyst recycle studies

While ionic liquids have been used as a means to immobilise and recycle polyoxometalate catalysts this approach is not always effective since product extraction can lead to leaching of the catalyst and gradual erosion in the conversion. Reasoning that the highly ionic microenvironment of polymer immobilised ionic liquids should efficiently retain the peroxotungstate during extraction, catalyst recycle experiments were undertaken using 0.5 mol% **3a** for the sulfoxidation of thioanisole to compare with the corresponding pyrrolidinium-based ROMP-derived [PO₄{WO(O₂)₂]₄]@PIILP system and to assess the potential for fabricating a continuous flow process. Ethanol was identified as the solvent of choice for recycle studies as it combines high selectivity and TOFs with environmentally green credentials. The reaction time was reduced from 15 min to 5 min for this study and the catalyst was recovered by filtration, washed with ethanol, dried and reused directly without being replenished or reconditioned. The data in Figure 5 shows that **3a** recycled efficiently over 5 runs with only a minor reduction in conversion and no significant change in sulfoxide selectivity; thereafter conversions dropped steadily although selectivity remained at 98% across all twelve runs.

Fig. 5 Recycle study for the sulfoxidation of thioanisole in ethanol catalysed by [PO₄{WO(O₂)₂]₄]@ImPIILP (**3a**).



Analysis of solvent collected during recovery of the catalyst from the first five runs revealed that the tungsten content was too low to be detected by ICP-OES (i.e. < 1 ppm), a strong indication that the peroxotungstate was efficiently retained by the polymer immobilised ionic liquid. Moreover, analysis of catalyst recovered after the fifth run gave a tungsten content of 30.6% which is similar to that of the unused catalyst, a further indication that leaching was negligible. The IR spectrum of **3a** contains bands at 1078 cm⁻¹ ν(P-O), 941 cm⁻¹, ν(W=O), 588 cm⁻¹, ν_{asym}(W-O₂) and 529 cm⁻¹, ν_{asym}(W-O₂), which is a close match to those reported for related systems.⁵¹ A sample of catalyst recovered after run five contained IR bands that were essentially superimposable on those of fresh catalyst and an SEM image of the sample showed no significant morphological changes, indicating that the peroxotungstate is stable and

remains intact under the reaction conditions; a copy of these IR spectra and the SEM image are provided in the ESI. The gradual erosion in conversion on successive recycles is thought to be due to attrition during the filtration and catalyst recovery procedure rather than deactivation as the mass of catalyst recovered after the 12th run (0.011 g) is significantly less than the initial mass of catalyst (0.026 g) used in the first run. To this end, the turnover number of 103 calculated using the mass of catalyst recovered after run 12 is close to that of 109 obtained in run 1.

Segmented and continuous flow

The efficacy of **3a** as a catalyst for the selective oxidation of sulfides under mild conditions coupled with the mechanical integrity of the system prompted us to extend catalyst testing to segmented and continuous flow protocols as this would allow straightforward product separation as well as scale-up and should overcome the catalyst attrition that occurred during the batch recycle studies.⁴⁵ In this regard, there have been surprisingly few reports of continuous flow sulfoxidation and as such there is a need to explore this technology to identify systems that operate under mild conditions and give high selectivity in short reaction times.

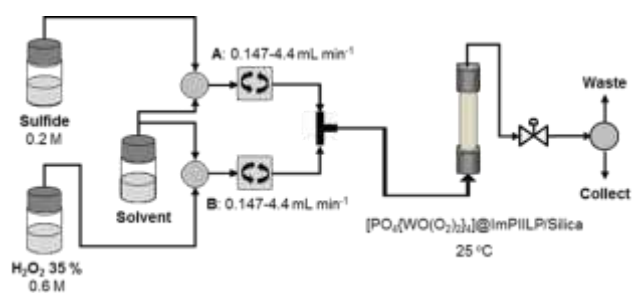


Fig. 6 Schematic representation of the reactor configuration for segmented and continuous flow sulfoxidation catalysed by $[\text{PO}_4\{\text{WO}(\text{O}_2)_2\}_4]\text{@ImPIILP}$ (**3a**).

The configuration of the flow system is shown in Figure 6 and is based on a Uniqsis FlowSyn reactor. Preliminary optimisation studies were conducted using a segmented flow set-up in which 1 mL aliquots of thioanisole (0.2 M) in ethanol and 30% hydrogen peroxide (0.2–0.6 M) were simultaneously pumped through a reactor cartridge packed with 2.0 g of silica (Geduran[®] Si60 43–60 μm) mixed with 0.1 g of $[\text{PO}_4\{\text{WO}(\text{O}_2)_2\}_4]\text{@ImPIILP}$ (**3a**) and using ethanol as the mobile phase; flow rates were varied with precise control between 0.146 and 8.8 mL min^{-1} , which correspond to residence times between 30 min and 0.5 min, respectively. The exiting product stream was collected in triplicate as 2 mL aliquots, subjected to an aqueous work-up and analysed by either ¹H or ¹³C NMR spectroscopy to determine the conversion and selectivity.

A survey of the effect of residence time (Rt) on selectivity and conversion as a function of the H_2O_2 :thioanisole ratio revealed that the optimum conversion-selectivity profile for the

sulfoxidation of thioanisole at 25 °C with ethanol as the mobile phase was obtained with 1.5 equiv. of H_2O_2 and a residence time of 10 min, details of which are shown in Figure 7a. Under these conditions, conversions increased gradually with increasing residence time from 8% for a residence time of 0.5 min to 88% when this was increased to 10 min and sulfoxide selectivity decreased slightly from 99% to 94% over the same time. Not surprisingly, when the reactor column was cooled to 0 °C longer residence times (< 60 min) were required to reach acceptable conversions, albeit with no improvement in selectivity which remained at 94%. Although good conversions were obtained at shorter residence times when the column was heated to 50 °C this was at the expense of sulfoxide selectivity which dropped below 90%; full details of the effect of temperature on the conversion-selectivity profile are provided in the ESI. Gratifyingly, the optimum conversion and sulfoxide selectivity compared favourably with that of 94% and 96% obtained in batch but with the advantage that a much lower H_2O_2 :substrate ratio is required. Moreover, the catalyst cartridge could be stored overnight and reused with only a minor reduction in performance indicating that the system may be stable and suitable for use in continuous flow (*vide infra*).

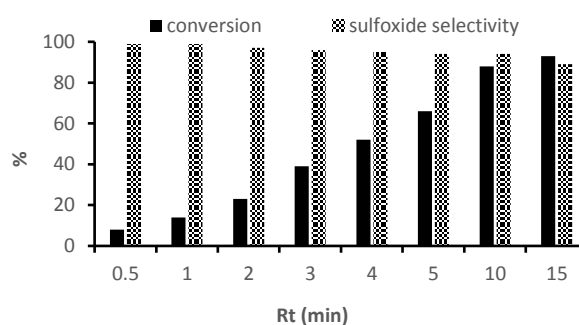


Fig. 7 Conversion-selectivity profile as a function of residence time (Rt) for the $[\text{PO}_4\{\text{WO}(\text{O}_2)_2\}_4]\text{@ImPIILP}$ -catalysed sulfoxidation of thioanisole in ethanol. Reaction conditions: 0.1 g catalyst/2.0 g silica, 1.5 equiv. 35% H_2O_2 , temp = 25 °C, residence time 0.5–15 min.

The high selectivity and conversion obtained for the sulfoxidation of dibenzothiophene in acetonitrile under batch conditions prompted us to explore the potential for developing a continuous flow process for oxidative desulfurization of crude oil as the overwhelming majority of studies involving ionic liquids have focused on batch extraction based protocols.⁵³ A survey of the conversion and selectivity as a function of residence time at 90 °C with acetonitrile as the mobile phase revealed that the concentration of sulfoxide peaked at a residence time of 2 min, after which sulfone selectivity increased rapidly with increasing conversion, ultimately reaching 96% at a residence time of 15 min (Fig. 8). These conditions are currently being applied to the oxidative desulfurisation of model crude oil to examine the feasibility of removing sulfur containing impurities under flow conditions.

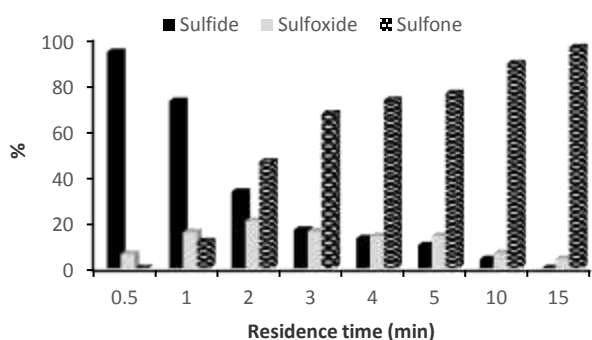


Fig. 8 Conversion-selectivity profile as a function of residence time (Rt) for the $[\text{PO}_4\{\text{WO}(\text{O}_2)_2\}_4]@\text{ImPIILP}$ -catalysed sulfoxidation of dibenzothiophene in acetonitrile. Reaction conditions: 0.1 g catalyst/2.0 g silica, 3 equiv. 35% H_2O_2 , MeCN, temp = 90 °C, residence time 0.5-15 min.

Encouraged by the promising conversion-selectivity profile achieved under segmented flow, a comparative continuous flow study was conducted using ethanol as the mobile phase; parallel reactions were also conducted with freshly prepared $[\text{NEt}_4]_3[\text{PO}_4\{\text{WO}(\text{O}_2)_2\}_4]$ and Merrifield resin-derived **3e** supported on silica as benchmarks. The continuous flow sulfoxidation of thioanisole was conducted by purging a catalyst column packed with a mixture of **3a** and silica with a 0.2 M solution of thioanisole in ethanol and a 0.3 M solution of peroxide at a rate of 0.44 mL min^{-1} ($R_t = 10 \text{ min}$) at 25 °C and monitored over an 8 hour period by sampling 5 mL aliquots in triplicate. The resulting performance-time profile in Figure 9a shows a slight decrease in conversion with time-on-stream from 87% to 76% while the sulfoxide selectivity remained relatively stable and constant at 92-94%. Interestingly, this conversion-selectivity profile is markedly more stable than its ROMP-derived counterpart in methanol which experienced a 30% drop in conversion and a concomitant reduction in sulfoxide selectivity from 77% to 53% after 8 h of continuous operation.^{41b} A comparative life-time study conducted using a reactor cartridge packed with $[\text{NEt}_4]_3[\text{PO}_4\{\text{WO}(\text{O}_2)_2\}_4]$ in silica was also undertaken to further assess the performance of our optimum POM@PIILP system. Under the same conditions $[\text{NEt}_4]_3[\text{PO}_4\{\text{WO}(\text{O}_2)_2\}_4]/\text{SiO}_2$ was highly active for the sulfoxidation of thioanisole in ethanol during the first hour after which conversions dropped quite dramatically with time such that the system was completely inactive after 3 h; this was associated with efficient leaching of the peroxotungstate as quantified by IPC analysis (Figure 9b). Having demonstrated that catalyst generated from in-house synthesised polymer immobilised ionic liquid outperformed that prepared from commercially available Merrifield resin modified with imidazolium ions for sulfoxidations conducted in batch, a performance-time profile was obtained to compare the efficiency of this system under continuous flow operation. Under the same conditions, a reactor column packed with Merrifield resin-derived **3e** on silica showed a steady decrease in conversion from 65% to 47% together a minor decrease in selectivity from 94% to 91% (Figure 9c). Although the drop in selectivity was relatively minor, the conversions are markedly lower than those obtained for **3a** under the same conditions

which highlights the advantages of developing polymer immobilised ionic liquid supports in house.

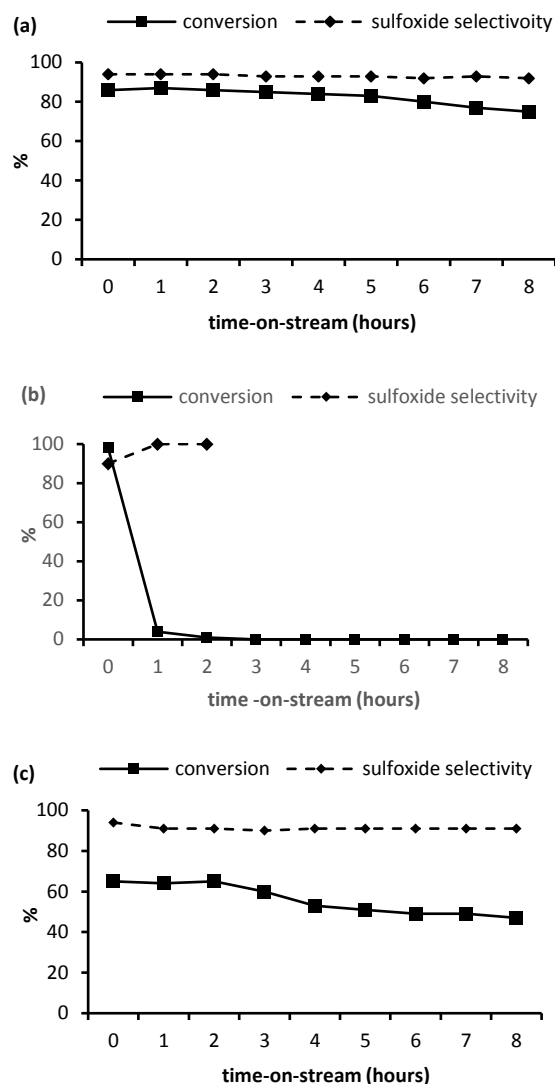


Fig. 9 Conversion-selectivity profile as a function of time-on-stream for continuous flow sulfoxidation of thioanisole catalysed by (a) $[\text{PO}_4\{\text{WO}(\text{O}_2)_2\}_4]@\text{ImPIILP}$ (**3a**), (b) $[\text{NBu}_4]_3[\text{PO}_4\{\text{WO}(\text{O}_2)_2\}_4]$ and (c) Merrifield-derived $[\text{PO}_4\{\text{WO}(\text{O}_2)_2\}_4]@\text{ImPIILP}$ (**3e**) each on silica using ethanol as the mobile phase and a residence time of 10 min (space velocity = 0.176 min^{-1}).

Finally, the reusability of the catalyst cartridge and the stable conversion-selectivity profile obtained under continuous flow prompted us to conduct a semi-quantitative scale-up and isolation experiment using ethanol as the mobile phase. Under optimum conditions 2.5 g of thioanisole was processed in 8 hours with a conversion of 82%, a sulfoxide selectivity of 92% and a total turnover number (TTNO) of 12,040; this is a marked and significant improvement on the 52% conversion obtained with ROMP-derived peroxotungstate-based $[\text{PO}_4\{\text{WO}(\text{O}_2)_2\}_4]@\text{PIILP}$ under similar conditions and in the same time.

Conclusion

Styrene based polymer immobilised ionic liquid supported peroxotungstates generated from in-house synthesised imidazolium-decorated styrene co-polymers as well as commercially available resins have been evaluated as catalysts for the selective sulfoxidation of sulfides and their performance compared against their ROMP-derived counterparts in order to assess the relative merits of each system. Within the limited range of catalysts tested, performance appears to depend on the nature of the substituents attached to the imidazolium ring with in-house prepared *N*-benzyl-based [PO₄{WO(O₂)₂]₄@ImPIILP outperforming its *N*-methyl counterparts as well as catalysts prepared from commercially available resins, in most cases by quite some margin. Interestingly, styrene-based [PO₄{WO(O₂)₂]₄@ImPIILP gave high sulfide selectivity in both acetonitrile and ethanol across the range of substrates examined; this is in stark contrast to their ROMP-based counterparts which gave markedly higher sulfoxide selectivities in alcohols compared with acetonitrile. Ethanol was identified as the solvent of choice for batch reactions on the basis that it gave the optimum balance of selectivity and conversion and is in the environmentally preferred class of solvent. The catalyst could be recovered in an operationally straightforward procedure and reused in five runs before conversions began to decrease. A segmented flow process based on a reactor cartridge packed with the optimum catalyst and silica gave high sulfoxide selectivities and good conversions at short residence times under mild conditions with ethanol as the mobile phase. The catalyst also operated efficiently and with a stable conversion-selectivity profile under continuous flow processing with ethanol as the carrier. Gratifyingly, the performance-time profile over 8h of continuous operation was significantly more stable with higher conversions and sulfoxide selectivities than that for the corresponding ROMP-derived system. We are currently exploring the imidazolium-substituent dependent performance of these systems in order to elucidate a composition-performance relationship and thereby identify an optimum catalyst-support combination. Future studies will aim to apply PIILP technology to a wider range of catalytic transformations as well as develop an understanding of how catalyst-support interactions influence efficiency, this will be achieved by; (i) introducing functionality onto the support to modify hydrophilicity and porosity in order to facilitate substrate access, improve recyclability and longevity under continuous flow operation and develop aqueous phase compatible systems, (ii) incorporating coordinating heteroatoms to develop new supported molecular catalysts and stabilize metal nanoparticles and (iii) designing novel architectures such as nanocapsules and polymeric micelles for use in catalysis.

Experimental Section

Poly-3-benzyl-1-(4-vinylbenzyl)-1H-imidazol-3-ium bromide-co-styrene (2a).

A flame-dried Schlenk flask was charged with AIBN (0.81 g, 4.9 mmol, 5 mol %) followed by 3-benzyl-1-(4-vinylbenzyl)-1H-

imidazol-3-ium bromide monomer **1a** (11.61 g, 32.8 mmol), styrene (6.8 mL, 66 mmol) and methanol (100 mL) and styrene (6.8 mL, 66 mmol) and the resulting mixture degassed with five freeze/pump/thaw cycles. After reaching ambient temperature the flask was heated to 70 °C and stirred for 72 hours. After this time the solution was allowed to cool, the volume reduced by half and the resulting concentrate added drop-wise into diethyl ether (600 mL) with rapid stirring. The product was isolated by filtration, washed with diethyl ether (3 x 50 mL) and dried under reduced pressure to afford polymer **2a** as a white solid (14.0 g, 76%). ¹H NMR (400 MHz, CDCl₃, δ): 9.67 (br, N-CH-N), 7.89 (br, Ar-H), 7.45 (br, Ar-H), 7.38 (br, Ar-H), 7.06 (br, Ar-H), 6.48 (br, Ar-H), 5.49 (br, Ar-CH₂-N), 5.38 (br, Ar-CH₂-N), 1.47 (br, CHCH₂, polymer backbone). FT-IR (neat, cm⁻¹): ν = 3406, 3057, 3025, 2925, 2850, 1601, 1558, 1493, 1452, 1149, 759, 700; Anal. Calc. for C₃₅H₃₅BrN₂ (563.6): C, 74.59; H, 6.26; N, 4.97 %. Found: C, 71.69; H, 6.72; N, 5.03%.

Poly-1,2-dimethyl-3-(4-vinylbenzyl)-1H-imidazol-3-ium chloride-co-styrene (2b).

Polymer **2b** was prepared and purified according to the procedure described above for **2a** and isolated as a white powder in 79% yield. ¹H NMR (400 MHz, CDCl₃, δ): 7.75 (br, Ar-H), 7.06 (br, Ar-H), 6.48 (br, Ar-H), 5.37 (br, Ar-CH₂-N), 3.79 (br, N-CH₃), 2.56 (br, N-CHCH₃-N), 1.48 (br, CHCH₂, polymer backbone). FT-IR (neat, cm⁻¹): ν = 3290, 3026, 2923, 2850, 1587, 1536, 1513, 1493, 1452, 1034, 761, 701; Anal. Calc. for C₃₀H₃₃ClN₂ (457.1): C, 78.83; H, 7.28; N, 6.13 %. Found: C, 73.52; H, 6.83; N, 6.57 %.

Synthesis of poly-1-methyl-3-(4-vinylbenzyl)-1H-imidazol-3-ium chloride-co-styrene (2c).

Polymer **2c** was prepared and purified according to the procedure described above for **2a** and isolated as a white powder in 59% yield. ¹H NMR (400 MHz, CDCl₃, δ): 9.51 (br, N-CH-N), 7.75 (br, Ar-H), 7.06 (br, Ar-H), 6.49 (br, Ar-H), 5.36 (br, Ar-CH₂-N), 3.87 (br, N-CH₃), 1.67 (br, CHCH₂, polymer backbone), 1.42 (br, CHCH₂, polymer backbone). FT-IR (neat, cm⁻¹): ν = 3343, 3142, 3056, 3025, 2924, 2849, 1601, 1572, 1493, 1452, 1160, 1031, 760, 700, 619; Anal. Calc. for C₂₉H₃₁ClN₂ (443.0): C, 78.62; H, 7.05; N, 6.32%. Found: C, 74.65; H, 6.76; N, 6.29 %.

Synthesis of imidazolium-decorated Merrifield resin (2e).

A flame-dried Schlenk flask was charged with imidazole loaded Merrifield resin (1.65 g) and benzyl bromide (2.38 mL, 20.0 mmol) in dry acetonitrile (20 mL) and the reaction mixture was allowed to stir for 72 hours. The reaction mixture was filtered and washed with acetonitrile (50 mL) and diethyl ether (100 mL) and the resulting solid dried under vacuum to afford the **2e** as a white solid (1.15 g). FT-IR (neat, cm⁻¹): ν = 3059, 3025, 2922, 2850, 1601, 1493, 1452, 1151, 1028, 756, 697; CHN Anal. Calc. based on measured loading of imidazole in 41 N, 2.33%. Found: C, 80.68; H, 7.97; N, 1.43%.

Polymer supported peroxophosphotungstate (3a).

Aqueous hydrogen peroxide solution (35% w/w, 10.2 mL, 118 mmol) was added to a solution of phosphotungstic acid (1.70 g, 600 μ mol) in water (1 mL) and the resulting mixture stirred at room temperature for 30 minutes. After this time, a solution of **2a** (1.00 g, 1.80 mmol) in ethanol (50 mL) was added and the reaction mixture stirred for a further 30 minutes after which it was added drop-wise into diethyl ether (500 mL) with rapid stirring. The product was isolated by filtration, washed with diethyl ether (3 \times 50 mL) and dried under reduced pressure to afford **3a** as an off white solid (1.00 g, 37%). FT-IR (neat, cm^{-1}): ν = 3140, 3061, 3026, 2925, 1712, 1640, 1602, 1558, 1494, 1453, 1148, 1029, 943, 887, 814, 756, 700; Anal. Calc. for $\text{C}_{105}\text{H}_{105}\text{N}_6\text{O}_{24}\text{PW}_4$ (2601.3) C, 48.48; H, 4.07; N, 3.23 %. Found: C, 47.45; H, 4.25; N, 3.01 %; 32.3 wt% tungsten and a peroxotungstate loading of 0.414 mmol g^{-1} .

Polymer supported peroxophosphotungstate (3b).

$[\text{PO}_4\{\text{WO}(\text{O}_2)_2\}_4]@\text{ImPIILP}$ **3b** was prepared and purified according to the procedure described above for **3a** and isolated as a white powder in 49% yield. FT-IR (neat, cm^{-1}): ν = 3408, 3140, 3026, 2926, 1614, 1493, 1452, 1422, 1078, 949, 820, 759, 701; Anal. Calc. for $\text{C}_{90}\text{H}_{99}\text{N}_6\text{O}_{24}\text{PW}_4$ (2415.1) C, 44.76; H, 4.13; N, 3.48 %. Found: C, 41.29; H, 4.05; N, 3.38 %; 33.9 wt% tungsten and a peroxotungstate loading of 0.464 mmol g^{-1} .

Polymer supported peroxophosphotungstate (3c).

$[\text{PO}_4\{\text{WO}(\text{O}_2)_2\}_4]@\text{ImPIILP}$ **3c** was prepared and purified according to the procedure described above for **3a** and isolated as a white powder in 29% yield. FT-IR (neat, cm^{-1}): ν = 3411, 3149, 3026, 2925, 1633, 1602, 1562, 1493, 1452, 1425, 1159, 1080, 1029, 956, 869, 836, 756, 700; Anal. Calc. for $\text{C}_{87}\text{H}_{93}\text{N}_6\text{O}_{24}\text{PW}_4$ (2373.0) C, 44.03; H, 3.95; N, 3.54 %. Found: C, 41.04; H, 3.99; N, 3.14 %; 35.0 wt% tungsten and a peroxotungstate loading of 0.479 mmol g^{-1} .

Peroxophosphotungstate loaded Amberlite (3d).

Aqueous hydrogen peroxide solution (35% w/w, 11.9 mL, 139 mmol) was added to a solution of phosphotungstic acid (2.00 g, 700 μ mol) in water (1.2 mL) and the resulting mixture stirred at room temperature for 30 minutes. After this time, the solution was passed through a narrow sinter funnel containing Amberlite IRA 900 chloride form (2.00 g). The Amberlite was then washed with water (50 mL) and Et_2O (50 mL) and the solvent removed under reduced pressure to afford the functionalised Amberlite as white beads. FT-IR (neat, cm^{-1}): ν = 3401, 3030, 2928, 2362, 2343, 1636, 1614, 1476, 924, 885, 715; Found: C, 44.91; H, 7.66; N, 3.81 %; 16.3 wt% tungsten and a peroxotungstate loading of 0.223 mmol g^{-1} .

Peroxophosphotungstate loaded imidazolium-decorated Merrifield resin (3e).

Aqueous hydrogen peroxide solution (35% w/w, 4.5 mL, 52 mmol) was added to a solution of phosphotungstic acid (0.75 g, 0.30 mmol) in water (0.5 mL) and the mixture was stirred at room temperature for 30 minutes. After this time, the solution was added to a suspension of **2e** (0.9 g) in ethanol (47 mL) and the mixture was stirred for a further 30 minutes after which it was added drop-wise into diethyl ether (500 mL) with rapid

stirring. The product was isolated by filtration, washed with diethyl ether (3 \times 50 mL) and finally dried under reduced pressure to afford **3e** as a white solid (1.2 g, 73%). FT-IR (neat, cm^{-1}): ν = 3059, 3026, 2922, 2850, 1716, 1602, 1558, 1493, 1452, 1148, 1029, 960, 814, 755, 697; Anal. Calc. for $\text{N}_6\text{O}_{24}\text{PW}_4$ N, 1.86 %. Found: C, 63.46; H, 6.16; N, 0.97 %; 30.2 wt% tungsten and a peroxotungstate loading of 0.413 mmol g^{-1} .

General procedure for catalytic sulfoxidation in batch.

A flame-dried Schlenk flask was allowed to cool to room temperature and charged with sulfide (1.0 mmol), catalyst (0.56-0.58 mol %) and solvent (3 mL). The reaction was initiated by the addition of aqueous hydrogen peroxide (35% w/w, 0.21 mL, 2.5 mmol) and allowed to stir at room temperature for 15 minutes. The reaction mixture was diluted with dichloromethane (25 mL), washed with water (50 mL) and the organic extract dried over MgSO_4 filtered and the solvent removed under reduced pressure. The resulting residue was analysed by either ^1H or $^{13}\text{C}\{^1\text{H}\}$ NMR spectroscopy to quantify the composition of starting material and products; for each substrate tested an internal standard of 1,3-dinitrobenzene was initially employed to ensure mass balance.

General procedure for the catalytic sulfoxidation recycle studies.

A PTFE centrifuge tube containing a magnetic stirrer bar was placed in a flame-dried Schlenk flask. The tube was charged with **3a** (0.01146 mmol, 0.58 mol %), sulfide (2.0 mmol) and solvent (6 mL) and stirred for 2 minutes. The reaction was initiated by the addition of aqueous hydrogen peroxide (35% w/w, 0.43 mL, 5.0 mmol) and allowed to stir at room temperature for 5 minutes. After this time the solution was centrifuged (5 min, 14,000 rpm), decanted and the remaining PIILP catalyst washed with the reaction solvent (6 mL), re-centrifuged and the solvent decanted. The reaction solution was diluted with dichloromethane (25 mL), washed with water (50 mL) and the organic extract dried over MgSO_4 filtered and the solvent removed under reduced pressure. The resulting residue was analysed by ^1H NMR spectroscopy to quantify the composition of starting material and products. The residue in the centrifuge tube was re-suspended in solvent and reused without any further treatment.

General procedure for the catalytic sulfoxidation kinetic studies.

A flame-dried Schlenk flask was allowed to cool to room temperature and charged with sulfide (4.0 mmol), **3a** (0.02 mmol, 0.5 mol %) and solvent (12 mL). The reaction was initiated by the addition of aqueous hydrogen peroxide (35% w/w, 0.86 mL, 10.0 mmol) and the resulting mixture stirred at room temperature for 24 hours during which time 0.2 mL aliquots were removed for work-up (as above) and analysed by ^1H NMR spectroscopy.

General procedure for segmented and continuous flow catalytic sulfoxidations.

Two reservoirs were charged with sulfide (5.0 mmol) dissolved in the appropriate solvent (25 mL, 0.2 M) and hydrogen

peroxide (35% w/w) in the same solvent (25 mL, 0.2–0.6 M). A Uniqsis FlowSyn reactor was used to pump 1.0 mL of each reagent at total flow rates that varied between 0.146 mL min⁻¹ and 8.8 mL min⁻¹ through a T-piece mixer to combine the two streams; in the case of segmented flow an additional reservoir of carrier solvent was also employed. The reaction stream was then flowed through a OMNIFIT® glass column reactor cartridge (10 mm id × 100 mm) packed with 0.1 g of [PO₄(WO₂)₂]₄@PIILP and 2.0 g of SiO₂ (Geduran® Si 60) and mounted in a FlowSyn column heater. The exiting stream was passed through a back pressure regulator (BPR) and 2 mL fractions were collected into separate vials followed by a 2 mL post-collect. Each sample was diluted with dichloromethane (10 mL), washed with water (ca. 15 mL), the organic extract dried over MgSO₄, the solvent removed under reduced pressure and the resulting residue analysed by ¹H NMR spectroscopy to quantify the composition of starting material and products.

Acknowledgements

We gratefully acknowledge Newcastle University for financial support (A. R. C. and J. R. E). Solid state P-31 and C-13 NMR spectra were obtained at the EPSRC UK national Solid State NMR Service at Durham University and high resolution mass spectra were obtained at the EPSRC National Mass Spectrometry Service in Swansea.

References

- (a) M. C. Carreno, *Chem. Rev.*, 1995, **95**, 1717–1760; (b) I. Fernandez and N. Khair, *Chem. Rev.*, 2003, **103**, 3651–3706; (c) S. Caron, R. W. Dugger, S. G. Ruggeri, J. A. Ragan and D. H. B. Ripin, *Chem. Rev.*, 2006, **106**, 2943–2989; (d) P. Metzner and A. Thuillier, *Sulfur Reagents in Organic Synthesis*, Academic Press, London, 1994; (e) Synthesis of Sulfones, Sulfoxides and Cyclic Sulfides, eds. S. Patai, Z. Rappoport, John Wiley: Chichester, U.K., 1994; (f) R. Bentley, *Chem. Rev.*, 2005, **105**, 609–624.
- L. Fernandez and N. Khair, *Chem. Rev.*, 2003, **103**, 3651–3705.
- (a) L. Du, P. Cao, J. Xing, Y. Lou, L. Jiang, L. Li and J. Liao, *Angew. Chem. Int. Ed.*, 2013, **52**, 4207–42011; (b) W.-Y. Qi, T.-S. Zhu and M.-H. Xu, *Org. Lett.*, 2011, **13**, 3410–3413; (c) S.-S. Jin, H. Wang and M.-H. Xu, *Chem. Commun.*, 2011, **47**, 7230–7232; (d) J. Chen, J.-M. Chen, F. Lang, X.-Y. Zhang, L.-F.; Cun, J.; Zhu, J.-G.; Deng and J. Liao, *J. Am. Chem. Soc.*, 2010, **132**, 4552–4553; (e) Q.-A. Chen, X. Dong, M.-W. Chen, D.-S. Wang, Y.-G. Zhou and Y.-X. Li, *Org. Lett.*, 2010, **12**, 1928–1931; (f) F. Lang, D.; Li, J.-M. Chen, J. Chen, L.-C. Li, L.-F. Cun, J. Zhu, J.-G. Deng and J. Liao, *Adv. Synth. Catal.*, 2010, **352**, 843–846.
- (a) H. Li, L. He, J. Lu, W. Zhu, X. Jiang, Y. Wang and Y. Tan, *Energy Fuels*, 2009, **23**, 1354–1357; (b) W. Zhu, H. Li, X. Jiang, Y. Yan, J. Lu, L. He and J. Xia, *Green Chem.*, 2008, **10**, 641–646; (c) L. He, H. Li, W. Zhu, J. Guo, X. Jiang, J. Lu and Y. Yan, *Ind. Eng. Chem. Res.*, 2008, **47**, 6890–6895; (d) H. Li, X. Jiang, W. Zhu, J. Lu, H. Shu and Y. Yan, *Ind. Eng. Chem. Res.*, 2009, **48**, 9034–9039; (e) W. Huang, W. Zhu, H. Li, H. Shi, G. Zhu, H. Li and G. Chen, *Ind. Eng. Chem. Res.*, 2010, **49**, 8998–9003; (f) Y. Ding, W. Zhu, H. Li, W. Jeng, M. Zhang, Y. Duan and Y. Chang, *Green Chem.*, 2011, **13**, 1210–1216; (g) W. Zhu, Y. Ding, H. Li, J. Qin, Y. Yanhong, J. Xiong and Y. Xu, H. Liu, *RSC Advances*, 2013, **3**, 3893–3898; (h) E. Lissner, W. F. de Souza, B. Ferrera and J. Dupont, *ChemSusChem*, 2009, **2**, 962–964.
- (a) N. K. Jana and J. G. Verkade, *Org. Lett.*, 2003, **5**, 3787–3790; (b) R. J. Griffin, A. Henderson, N. J. Curtin, A. Echaliier, J. A. Endicott, I. R. Hardcastle, D. R. Newell, N. E. M. Noble, L. Z. Wang and B. T. Golding, *J. Am. Chem. Soc.*, 2006, **128**, 6012–6013.
- R. S. Varma and K. P. Naicker, *Org. Lett.*, 1999, **1**, 189–192.
- N. Fukuda and T. Ikemoto, *J. Org. Chem.*, 2010, **75**, 4629–4631.
- R. S. Varma, R. K. Saini and H. M. Meshram, *Tetrahedron Lett.*, 1997, **38**, 6525–6528.
- B. Yu, A. H. Liu, L. N. He, B. Li, Z. F. Diao and Y. N. Li, *Green Chem.*, 2012, **34**, 957–962.
- J. G. W. Gokel, H. M. Gerdes and D. M. Dishong, *J. Org. Chem.*, 1980, **45**, 3634–3639.
- P. Hanson, R. A. A. J. Hendrickx and J. R. L. Smith, *New J. Chem.*, 2010, **34**, 65–84.
- (a) R. A. Sheldon, *Chem. Ind. (London, UK)*, 1997, 12–15; (b) R. A. Sheldon, *Green Chem.* 2007, **9**, 1273–1283; (c) R. A. Sheldon *Chem. Commun.* 2008, 3352–3365.
- M. A. Rezvani, A. F. Shojaie, M. H. Loghmani, *Catal. Commun.* 2012, **25**, 36–40.
- (a) J. Legros and C. Bolm, *Angew. Chem. Int. Ed.*, 2003, **42**, 5487–5489; (b) J. Legros and C. Bolm, *Angew. Chem. Int. Ed.*, 2004, **43**, 4225–4228; (c) M. Bagherzadeh and M. Amini, *Inorg. Chem. Commun.* 2009, 21–25; (d) H. Egami and T. Katsuki, *J. Am. Chem. Soc.*, 2007, **129**, 8940–4941; (e) B. Li, A.-H. Liu, L.-N. He, Z.-Z. Yang, J. Gao and K.-H. Chen, *Green Chem.*, 2012, **14**, 130–135.
- (a) M. Bagherzadeh, R. Latifi, L. Tahsini and M. Amini, *Catal. Commun.*, 2008, **10**, 196–200; (b) M. Bagherzadeh, L. Tahsini and R. Latifi, *Catal. Commun.*, 2008, **9**, 1600–1609; (c) F. Xie, Z. Fu, H. S. Zhong, Z. P. Ye, X. P. Zhou, F. L. Liu, C. Y. Rong, L. Q. Mao and D. L. Yin, *J. Mol. Cat. A: Chemical*, 2009, **307**, 93–97.
- (a) A. V. Anisimov, E. V. Fedorova, A. Z. Lesnugin, V. M. Senyavi, L. A. Aslanov, V. B. Rybakov and A. V. Tarakanova, *Catal. Today*, 2003, **78**, 319–325; (b) V. Conte, F. Fabbianesi, B. Floris, P. Galloni, D. Sordi, I. W. C. E. Arends, M. Bonchio, D. Rehder and D. Bogdal, *Pure Appl. Chem.*, 2009, **81**, 1265–1277; (c) S. Barroso, P. Adao, F. Madeira, M. T. Duarte, J. C. Pessoa and A. M. Martins, *Inorg. Chem.*, 2010, **49**, 7452–7463.
- (a) A. M. Cojocariu, P. H. Mutin, E. Dumitriu, F. Fajula, A. Vioux and V. Hulea, *Chem. Commun.*, 2008, 5357–5359; (b) M. Mba, L. J. Prins, C. Zonta, M. Cametti, A. Valkonen, K. Rissanen and G. Licini, *Dalton Trans.*, 2010, **39**, 7384–7392; (c) W. Al-Maksoud, S. Daniele and A. B. Sorokin, *Green Chem.*, 2008, **10**, 447–451; (d) S. K. Karmee, L. Greiner, A. Kraynov, T. E. Müller, B. Niemeijera and W. Leitner, *Chem. Commun.*, 2010, 6705–6707; (e) L. Postigo, M. Ventura, T. Cuenca, G. Jiménez and B. Rayo, *Catal. Sci. Technol.* 2015, **5**, 320–324.
- T. Soundiressane, S. Selvakumar, S. Menage, O. Hamelin, M. Fontecave and A. P. Singh *J. Mol. Cat A: Chemical*, 2007, **270**, 132–143.
- (a) C. Yang, Q. P. Jin, H. Zhang, J. Liao, J. Zhu, B. Yu and J. G. Deng, *Green Chem.*, 2009, **11**, 1401–1405; (b) R. D. Chakravarthy, V. Ramkumar and D. K. Chand, *Green Chem.*, 2014, **16**, 2190–2196; (c) K. Jeyakumar and D. K. Chand, *Tetrahedron Lett.*, 2006, **47**, 4573–4576; (d) T. Cavattoni, T. D. Giacco, O. Lanzalunga, M. Mazzonna and P. Mencarelli, *J. Org. Chem.*, 2013, **78**, 4886–4894; (e) P. W. Davies and S. J.-C. Albrecht, *Angew. Chem. Int. Ed.*, 2009, **48**, 8372–8375; (f) G. P. Romanelli, P. I. Villabrilie, C. V. Cáceres, P. G. Vázquez and P. Tundo, *Catal. Commun.*, 2011, **12**, 726–730.
- (a) M. Ciclosi, C. Dinoi, L. Gonsalvi, M. Peruzzini, E. Manoury and R. Poli, *Organometallics*, 2008, **27**, 2281–2286; (b) X. Xue, W. Zhao, B. Ma and Y. Ding, *Catal. Commun.*, 2012, **29**, 73–76;

- (c) K. Kamata, T. Hirano and N. Mizuno, *Chem Commun.*, 2009, 3958–3960.
- 21 M. Kirihara, J. Yamamoto, T. Naguchi and Y. Hirai, *Tetrahedron Lett.* 2009, **50**, 1180–1183.
- 22 (a) J. Rudolph, K. L. Reddy, J. P. Chiang and K. B. Sharpless, *J. Am. Chem. Soc.*, 1997, **119**, 6189–6190; (b) W. A. Herrmann, R. M. Kratzer, H. Ding, W. R. Thiel and H. Glas, *J. Organomet. Chem.*, 1998, **555**, 293–295; (c) H. Adolfsson, C. Copéret, J. P. Chiang and A. K. Yudin, *J. Org. Chem.*, 2000, **65**, 8651–8658; (d) S. Yamazaki, *Org. Biomol. Chem.*, 2010, **8**, 2377–2385; (e) P. Altmann, M. Cokoja and F. E. Kühn, *Eur. J. Inorg. Chem.*, 2012, 3235–3239.
- 23 (a) J.-B. Feng, J.-L. Gong and X.-F. Wu, *RSC Adv.*, 2014, **4**, 29273–29275; (b) X.-F. Wu, *Tetrahedron Lett.*, 2012, **53**, 4328–4331.
- 24 (a) A. Corma, L. T. Nemeth, M. Renz and S. Valencia, *Nature*, 2001, **412**, 423–425; (b) H. Y. Luo, L. Bui, W. R. Gunther, E. Min and Y. Román-Leshkov, *ACS Catal.*, 2012, **2**, 2695–2699; (c) A. Corma, M. T. Navarro, L. Nemeth and M. Renz, *Chem. Commun.*, 2001, 2190–2191.
- 25 (a) A. Conde, L. Vilella, D. Balcells, M. M. Díaz-Requejo, A. Lledós and P. J. Pérez, *J. Am. Chem. Soc.*, 2013, **135**, 3887–3896; (b) O. Perraud, A. B. Sorokin, J.-P. Dutasta and A. Martinez, *Chem. Commun.*, 2013, **49**, 1288–1290; (c) A. M. Kirillov, M. N. Kopylovich, M. V. Kirillova, E. Y. Karabach, M. Haukka, M. F. C. Guedes da Silva and A. J. L. Pombeiro, *Adv. Synth. Catal.*, 2006, **348**, 159–174.
- 26 P. T. Anastas, J. C. Warner in *Green Chemistry: Theory and Practise*, Oxford University Press, New York, 1998.
- 27 (a) B. Karimi and M. Khorasani, *ACS Catalysis*, 2013, **3**, 1657–1664; (b) X.-Y. Shi and J.-F. Wei, *J. Mol. Catal. A: Chemical*, 2008, **280**, 142–147; (c) X. Shi, X. Han, W. Ma, J. Wei, J. Li, Q. Zhang and Z. Chen, *J. Mol. Catal. A: Chemical*, 2008, **341**, 57–62; (d) S. P. Das, J. J. Boruah, N. Sharma and N. S. Islam, *J. Mol. Catal. A: Chemical*, 2012, **356**, 36–45; (e) B. Karimi, M. Ghoreishi-Nezhad and J. H. Clark, *Org. Lett.*, 2005, **7**, 625–628; (f) F. Rajabi, S. Naserian, A. Primo and R. Luque, *Adv. Synth. Catal.*, 2011, **353**, 2060–2066; (g) J. J. Boruah, S. P. Das, S. R. Ankireddy, S. R. Gogoi and N. S. Islam, *Green Chem.*, 2013, **15**, 2944–2959; (h) B. Karimi, M. Khorasani, F. B. Rostami, D. Elhamifar and H. Vali, *ChemPlusChem* 2015, **80**, 990–999.
- 28 K. Liu, Z. Yao and Y.-F. Song, *Ind. Eng. Chem. Res.*, 2015, **54**, 9133–9141.
- 29 S. Doherty *Homogenous Catalysis in Ionic Liquids in Catalysis in Ionic Liquids: From Catalyst Synthesis to Application*, eds. C. Hardacre and V. Parvulescu, RSC Catalysis Series, 2014 pp 44–308.
- 30 C. J. Carrasio, F. Montilla, L. Bobadilla, S. Ivanova, J. A. Odriozola and A. Galindo, *Catal. Today* 2015, **255**, 102–108.
- 31 A. Pourjavadi, S. H. Hosseini, F. M. Moghaddam, B. Koushki and C. Bennett, *Green Chem.*, 2013, **15**, 2913–2919.
- 32 Y.-L. Hu, X.-B. Liu and D. Fang, *Catal. Sci. Technol.*, 2014, **4**, 38–42.
- 33 X. Shi, X. Han, W. Ma, J. Wei, J. Li, Q. Zhang and Z. Chen, *J. Mol. Catal. A: Chemical*, 2011, **341**, 57–62.
- 34 P. Zhao, M. Zhang, Y. Wu and J. Wang, *Ind. Eng. Chem. Res.*, 2012, **51**, 6641–6647.
- 35 S. Wang, L. Wang, M. Đaković, Z. Popović, H. Wu and Y. Liu, *ACS Catal.*, 2012, **2**, 230–237.
- 36 (a) B. Zhang, M.-D. Zhou, M. Cokaja, J. Mink, S.-L. Zang and F. E. Kuhn, *RSC Advances*, 2012, **2**, 8416–8420; (b) F. Liu, Z. Fu, Y. Liu, C. Lu, Y. Wu, F. Xie, Z. Ye, X. Zhou and D. Yin, *Ind. Eng. Chem. Res.*, 2010, **49**, 2533–2536.
- 37 Y.-L. Hu, D. Fang and R. Xing, *RSC Adv.*, 2014, **4**, 51140–51145.
- 38 (a) E. Rafiee and F. Mirnezami, *J. Mol. Liquids*, 2014, **199**, 156–161.
- 39 (a) M. Li, M. Zhang, A. Wei, W. Zhu, S. Xun, Y. Li, H. Li and H. Li, *J. Mol. Catal. A: Chemical*, 2015, **406**, 23–30; (b) X.-Y. Shi and J.-F. Wei, *J. Mol. Catal. A: Chemical*, 2008, **280**, 142–147.
- 40 A. Pourjavadi, M. Nazir-Chamazkoti and S. H. Hosseini, *New J. Chem.*, 2015, **39**, 1348–1354.
- 41 (a) S. Doherty, J. G. Knight, J. R. Ellison, D. Weekes, R.W. Harrington, C. Hardacre and H. Manyar, *Green Chem.*, 2012, **14**, 925–929; (b) S. Doherty, J. G. Knight, M. A. Carroll, J. R. Ellison, S. J. Hobson, S. Stevens, C. Hardacre and P. Goodrich, *Green Chem.*, 2015, **17**, 1559–1571.
- 42 (a) A. Casado-Sanchez, R. Gomez-Ballesteros, F. Tato, F. J. Soriano, G. Pascual-Coca, S. Cabrera, J. Aleman, *Chem. Commun.* 2016, DOI:10.1039/c6cc02452a. For additional examples of photocatalytic oxidation of sulfides see (b) X. Gu, X. Li, Y. Chai, Q. Yang, P. Li, Y. Yao, *Green Chem.* 2013, **15**, 357–361; (c) S. M. Bonesi, I. Manet, M. Freccero, M. Fagnoni, A. Albini, *Chem. Eur. J.* 2006, **12**, 4844–4857.
- 43 (a) C. Venturello and R. D’Aloisio, *J. Org. Chem.*, 1998, **53**, 1553–1557; (b) C. Venturello and R. D’Aloisio, *J. Mol. Catal.*, 1985, **32**, 107–110; (c) Y. Ishii, Y. Yamawaki, T. Ura, H. Yamada, T. Yoshida and M. Ogawa, *J. Org. Chem.*, 1988, **53**, 3587–3593; (d) R. Neumann and A. M. Khenkin, *J. Org. Chem.*, 1994, **59**, 7577–7579; (e) A. L. Salles, C. Aubry, R. Thouvenot, F. Robert, C. Doremieux-Morin, G. Chottard, H. Ledon, Y. Jeannin and J.-M. Bregeault, *Inorg. Chem.*, 1994, **33**, 871–878.
- 44 D. C. Duncan, R. C. Chambers, E. Hecht and C. L. Hill, *J. Am. Chem. Soc.*, 1995, **117**, 681–691.
- 45 (a) L. Vaccaro, D. Lanari, A. Marrocchi and G. Strappaveccia, *Green Chem.*, 2014, **16**, 3680–3704; (b) T. Noël and S. L. Buchwald, *Chem. Soc. Rev.*, 2011, **40**, 5010–5029; (c) C. G. Frost and L. Mutton, *Green Chem.*, 2010, **12**, 1687–1703; (d) V. Hessel, D. Kralisch, N. Kockmann, T. Noel and Q. Wang, *ChemSusChem*, 2013, **6**, 746–789; (e) J. Wegner, S. Ceylan and A. Kirschning, *Chem. Commun.*, 2011, **47**, 4583–4592; (f) C. J. Smith, N. Nikbin, S. V. Ley, H. Lange and I. R. Baxendale, *Org. Biomol. Chem.*, 2011, **9**, 1938–1947.
- 46 S. Meninno, A. Parrella, G. Brancatelli, S. Geremia, C. Gaeta, C. Talotta, P. Neri and A. Lattanzi, *Org. Lett.*, 2015, **17**, 5100–5103.
- 47 Y. Wang, K. Kamata, R. Ishimoto, Y. Ogasawara, K. Suzuki, K. Yamaguchi, N. Mizuno, *Catal. Sci. Technol.*, 2015, **5**, 2602–2611.
- 48 (a) F. Gregori, I. Nobili, F. Bigi, R. Maggi, G. Predieri and G. Sartori *J. Mol. Catal. A: Chemical*, 2008, **286**, 124–127; (b) E. Baciocchi, M. F. Gerini and A. Lapi, *J. Org. Chem.*, 2004, **69**, 3586–3589; (c) B. M. Choudary, B. Bharathi, Ch. V. Reddy and M. L. Kantam, *J. Chem. Soc. Perkin Trans.*, 2002, **1**, 2069–2074; (d) T. Patonay, W. Adam, A. Levai, P. Kover, M. Nemeth, E.-M. Peters and K. Peters, *J. Org. Chem.*, 2001, **66**, 2275–2280; (e) S. K. Maiti, S. Banerjee, A. K. Mukherjee, K. M. A. Malik and R. Bhattacharyya, *New J. Chem.*, 2005, **29**, 554–563.
- 49 (a) V. Hulea, A.-L. Maciucă, F. Fajula and E. Dumitriu *Appl. Catal. A: General*, 2006, **313**, 200–207; (b) A. L. Maciucă, C. E. Ciocan, E. Dumitriu, F. Fajula and V. Hulea, *Catal. Today*, 2008, **138**, 33–37; (c) M. Bonchio, V. Conti, M. A. De Conciliis, F. Di Furia, F. P. Ballistreri, G. A. Tomaselli and R. M. Toscano, *J. Org. Chem.*, 1995, **60**, 4475–4480.
- 50 B. Zhu, L.-K. Yan, W. Guan and Z.-M. Su, *Dalton Trans.*, 2015, **44**, 9063–9070.
- 51 (a) N. J. Cambell, A. C. Dengal, C. J. Edwards and W. P. Griffith, *J. Chem. Soc. Dalton Trans.*, 1989, 1203–1207; (b) A. J. Bailey, W. P. Griffith and B. C. Parkin, *J. Chem. Soc. Dalton Trans.*, 1995, 1833–1837; (c) A. C. Dengel, W. P. Griffith and B. C. Parkin, *J. Chem. Soc. Dalton Trans.*, 1993, 2683–2688; (d) E. Radkov and R. H. Beer, *Polyhedron*, 1995, **14**, 2139–2143; (e) C. Rocchiccioli-Deltcheff, M. Fournier, R. Franck and R. Thouvenot, *Inorg. Chem.*, 1983, **22**, 207–216.
- 52 (a) H. Li, L. He, J. Lu, W. Zhu, X. Jiang, Y. Wang and Y. Tan, *Energy & Fuels*, 2009, **23**, 1354–1357; (b) W. Zhu, H. Li, X. Jiang, Y. Yan, J. Lu, L. He and J. Xia, *Green Chem.*, 2008, **10**, 641–646; (c) L. He, H. Li, W. Zhu, J. Guo, X. Jiang, J. Ldu and Y. Yan, *Ind. Eng. Chem. Res.*, 2008, **47**, 6890–6895; (d) H. Li, X. Jiang, W. Zhu, J. Lu, H. Shu and Y. Yan, *Ind. Eng. Chem. Res.*,

2009, **48**, 9034–9039; (e) D. Xu, W. Zhu, H. Li, J. Zhang, F. Zou, H. Shi and Y. Yan, *Energy & Fuels*, 2009, **23**, 5929–5933; (f) W. Huang, W. Zhu, H. Li, H. Shi, G. Zhu, H. Li and G. Chen, *Ind. Eng. Chem. Res.*, 2010, **49**, 8998–9003; (g) J. Xu, S. Zhao, W. Chen, M. Wang and Y.-F. Song, *Chem. Eur. J.*, 2012, **18**, 4775–4781; (h) W. Zhu, J. Zhang, H. Li, Y. Chao, W. Jiang, S. Yin and H. Liu, *RSC Adv.* 2012, **2**, 658–664.